

Supplementary Materials for

Ruminococcin C, a promising antibiotic produced by a human gut symbiont

Steve Chiumento, Clarisse Roblin, Sylvie Kieffer-Jaquinod, Sybille Tachon, Chloé Leprêtre, Christian Basset, Dwi Adityarini, Hamza Olleik, Cendrine Nicoletti, Olivier Bornet, Olga Iranzo, Marc Maresca, Renaud Hardré, Michel Fons, Thierry Giardina, Estelle Devillard, Françoise Guerlesquin, Yohann Couté, Mohamed Atta, Josette Perrier, Mickael Lafond*, Victor Duarte*

*Corresponding author. Email: mickael.lafond@univ-amu.fr (M.L.); victor.duarte@cea.fr (V.D.)

Published 25 September 2019, *Sci. Adv.* **5**, eaaw9969 (2019)
DOI: 10.1126/sciadv.aaw9969

The PDF file includes:

Supplementary Methods

Fig. S1. Multi-alignment of RumMc radical SAM enzymes.

Fig. S2. Tandem mass spectra of RumC2-5 purified from cecal contents.

Fig. S3. Gene expression in the gut of rats monoassociated with *R. gnavus* E1 and heterologous expression and purification of MBP-mRumC1, mRumC1, and RumPc.

Fig. S4. Tandem mass spectra of N- and C-terminal fragments of RumC1 peptide present in in vivo and in vitro samples.

Fig. S5. Tandem mass spectra of mRumC1 mutants from which the residues involved in each thioether bridge were attributed.

Fig. S6. Determination of the connectivity of the thioether linkages in RumC1 by NMR.

Fig. S7. Cleavage of the leader N-terminal peptides of mRumC1 and anti-*Cp* activity assays.

Fig. S8. Evaluation of the ability of RumC1 to insert into bacterial lipids.

Fig. S9. Bacterial cytological profiling against *Cp*.

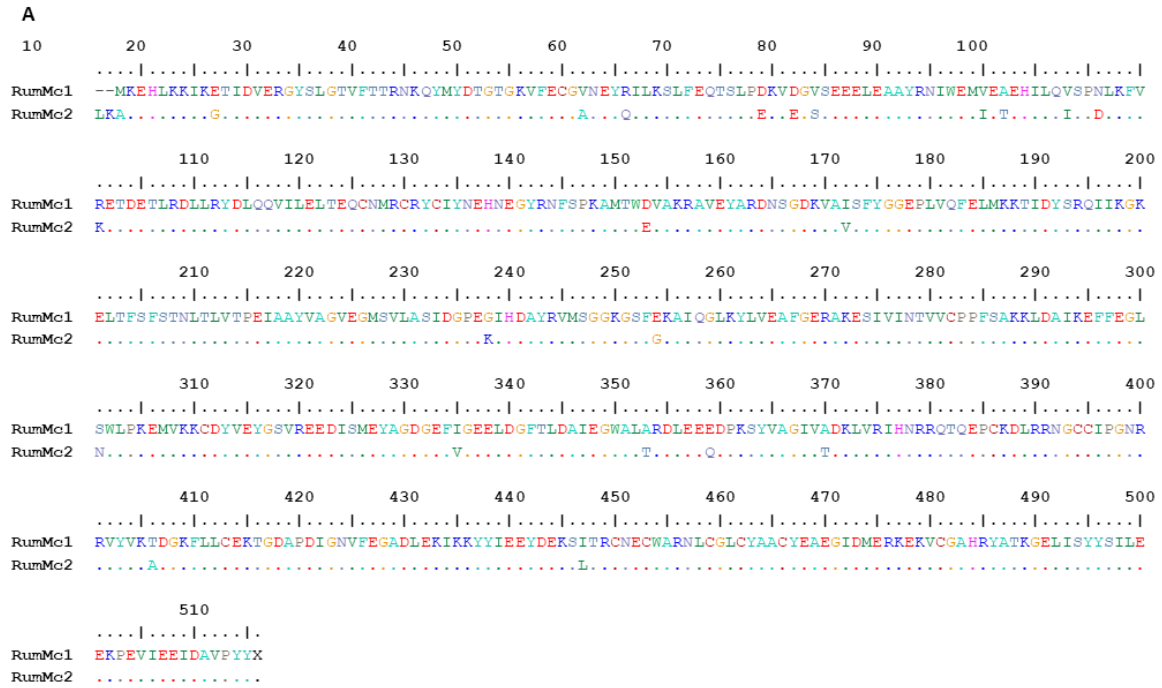
Fig. S10. Assessing RumC1 safety.

References (58, 59)

Other Supplementary Material for this manuscript includes the following:

(available at advances.sciencemag.org/cgi/content/full/5/9/eaaw9969/DC1)

Table S1 (Microsoft Excel format). Theoretical and experimental spectra lists.



B

Primer Name	Sequence (5'-3')	Target gene	Mutations	Application for
qPCR-rpoB-F	GGGGAAGAACTGGAGAACGTA	<i>rpoB</i>		RT-qPCR
qPCR-rpoB-R	TTCATATCAGGAGCGAAATC	<i>rpoB</i>		RT-qPCR
qPCR-C1-F	GGGATGTGTTTGTAGTGGAAAGC	<i>rumC1</i>		RT-qPCR
qPCR-C1-R	GCCGTTTTGCGACATTTGC	<i>rumC1</i>		RT-qPCR
qPCR-C2-F	GGTGGATGTAAATGCAGTGGC	<i>rumC2</i>		RT-qPCR
qPCR-C2-R	CACTCCGTTGTTCCACAGTAT	<i>rumC2</i>		RT-qPCR
qPCR-Mc1-F	AACTGGATGCGATCAAGGAG	<i>rumMc1</i>		RT-qPCR
qPCR-Mc1-R	AACGTGAAACCGTCCAGTTC	<i>rumMc1</i>		RT-qPCR
qPCR-Mc2-F	TGTTCTGGCAAGCATAGACG	<i>rumMc2</i>		RT-qPCR
qPCR-Mc2-R	CACTAAATGGCGGACAGACC	<i>rumMc2</i>		RT-qPCR
qPCR-Pc-F	GAGACCATCGGAGACGAGTG	<i>rumPc</i>		RT-qPCR
qPCR-Pc-R	TCACTGTCCGAATTTCTTTCC	<i>rumPc</i>		RT-qPCR
Mut-C1-C3A-F	CAAGTGGGGTGCCGTGTGCAGCG	<i>rumC1</i>	C3A	Site directed mutagenesis of mRumC1
Mut-C1-C3A-R	CTGCCCTCGAAGTCCGCA	<i>rumC1</i>	C3A	Site directed mutagenesis of mRumC1
Mut-C1-C5A-F	GGGTTGCGTGCCAGCGGTAGCA	<i>rumC1</i>	C5A	Site directed mutagenesis of mRumC1
Mut-C1-C5A-R	CACTTGCTGCCCTCGAAG	<i>rumC1</i>	C5A	Site directed mutagenesis of mRumC1
Mut-C1-C22A-F	TCCGGCGTACGCCGTGGTTATTG	<i>rumC1</i>	C22A	Site directed mutagenesis of mRumC1
Mut-C1-C22A-R	CCCCTGTTATGGCTGTTT	<i>rumC1</i>	C22A	Site directed mutagenesis of mRumC1
Mut-C1-C26A-F	CGTGGGTTATGCCGCAACAACGGTGTGG	<i>rumC1</i>	C26A	Site directed mutagenesis of mRumC1
Mut-C1-C26A-R	CAGTACGCCGACCCGCG	<i>rumC1</i>	C26A	Site directed mutagenesis of mRumC1

Fig. S1. Multi-alignment of RumMc radical SAM enzymes. (A) Alignment of RumMc1 and RumMc2. Conserved residues are marked ".", small and small + hydrophobic (including aromatic -Y) residues are in red, acidic amino acids are in blue, basic amino acids in magenta, hydroxyl + sulfhydryl + amine + G amino acids are green and unusual amino/imino acids are in grey. Alignment of the five RumC peptide isoforms. **(B) Primers used in this study.** All primer sets used for RT-qPCR displayed good efficiency (between 87 and 100%).

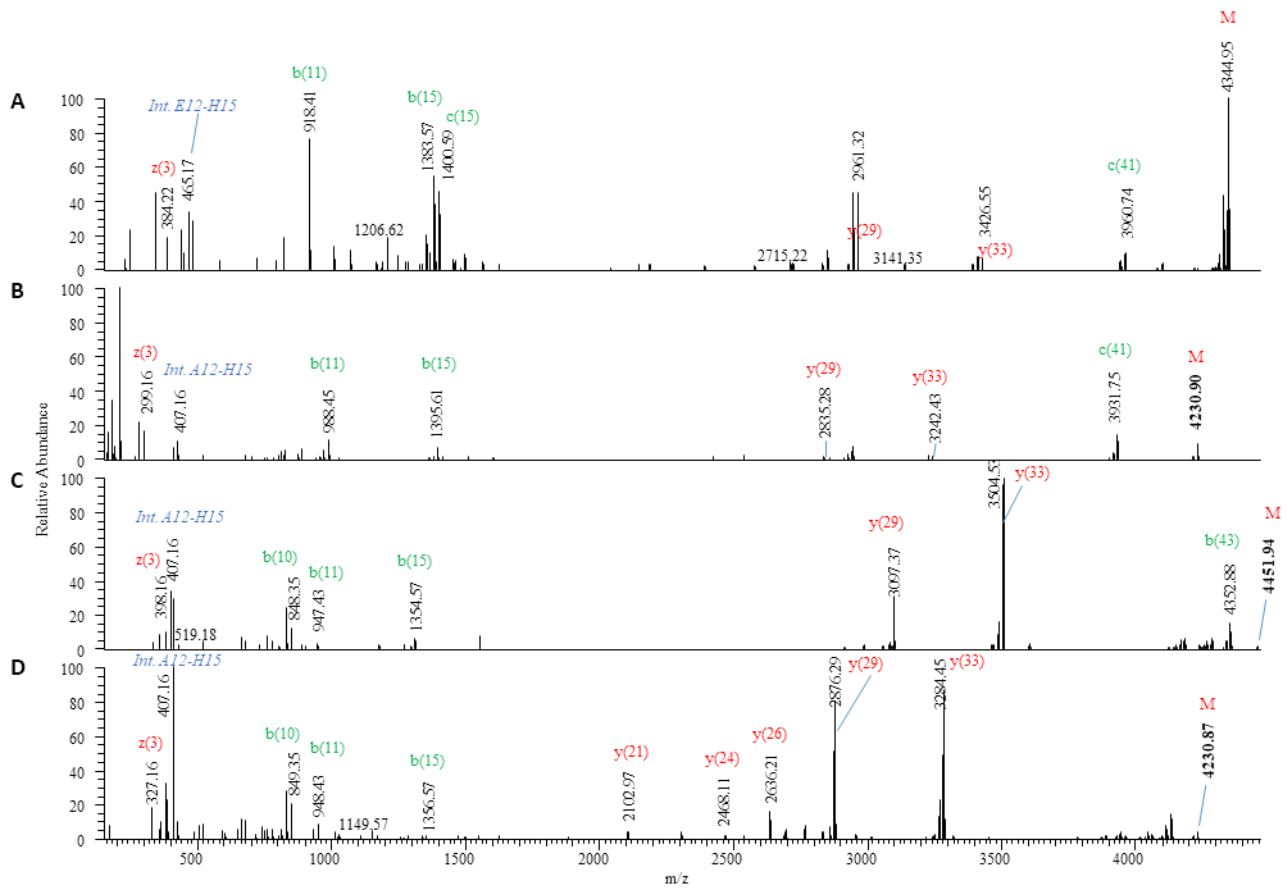


Fig. S2. Tandem mass spectra of RumC2-5 purified from cecal contents. Deconvoluted MS/MS spectra of (A) RumC2 peptide eluting at 18' with an $m/z = (1087.24)^{4+}$, (B) RumC3 peptide eluting at 22.5' with an $m/z = (1058.728)^{4+}$, (C) RumC4 peptide eluting at 20' with an $m/z = (1113.99)^{4+}$, and (D) RumC5 peptide eluting at 23' with an $m/z = (1058.722)^{4+}$. As observed for RumC1, these spectra reveal characteristic fragmentation patterns due to the presence of four thioether bonds in each mature peptide.

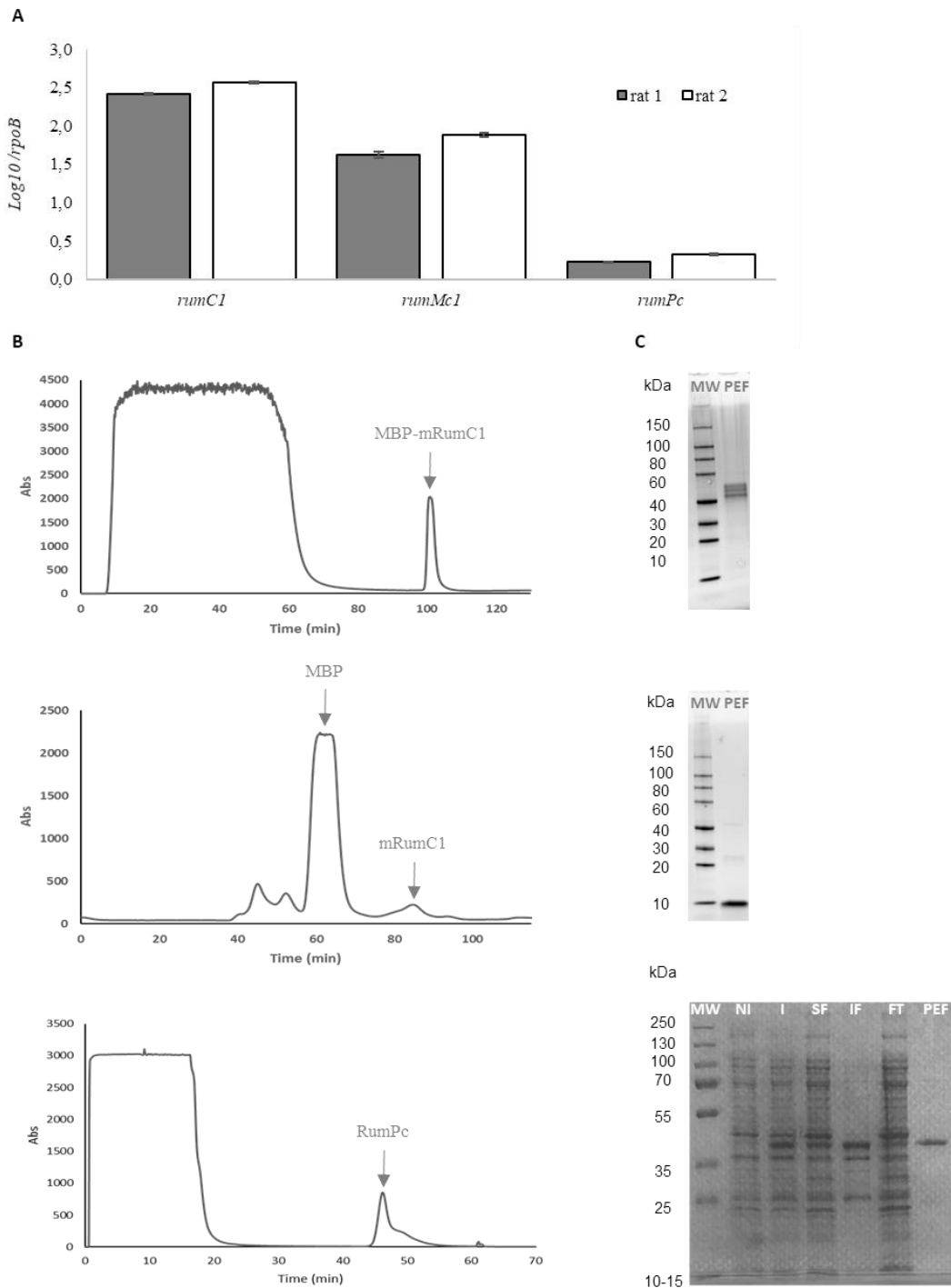


Fig. S3. Gene expression in the gut of rats monoassociated with *R. gnavus* E1 and heterologous expression and purification of MBP-mRumC1, mRumC1, and RumPc. (A) mRNA transcripts were purified from caecal contents of rats mono-associated with *R. gnavus* E1. Expression levels were measured for genes encoding the peptide RumC1, the sactisynthase RumMc1 and the peptidase RumPc. Expression levels for the genes of interest were normalised against expression of *rpoB*. **(B)** FPLC chromatograms of overexpressed MBP-mRumC1 (top), mRumC1 (middle) and RumPc (bottom). **(C)** SDS-PAGE analysis of purified MBP-mRumC1 (top), mRumC1 (middle) and RumPc (bottom). NI: Non-induced culture, I: Induced culture, SF: Soluble Fraction, IF: Insoluble Fraction, FT: FlowThrough and PEF: Pool of Eluted Fractions.

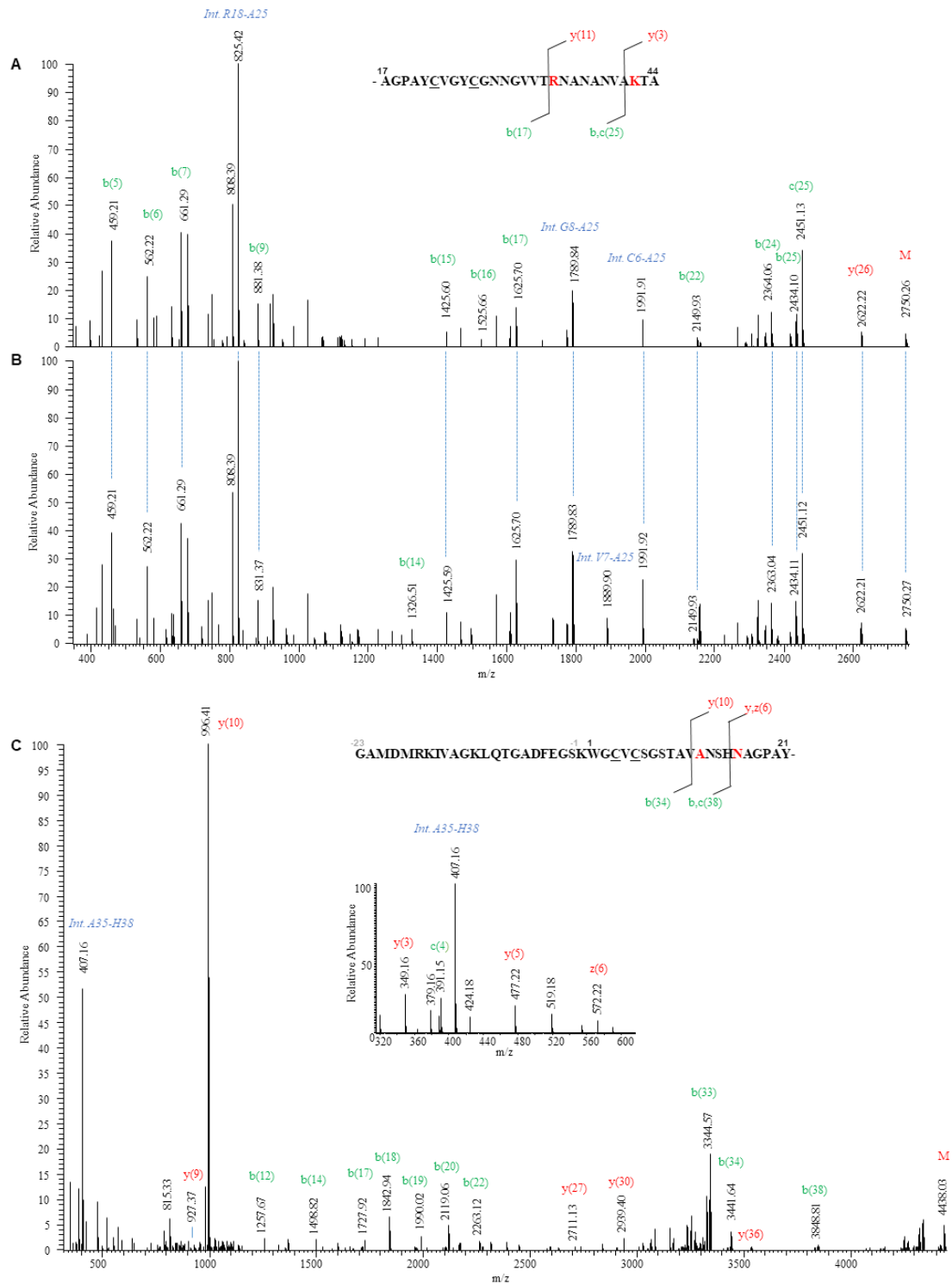


Fig. S4. Tandem mass spectra of N- and C-terminal fragments of RumC1 peptide present in in vivo and in vitro samples. (A) Deconvoluted MS/MS spectrum of a C-terminal fragment of the in vivo-produced RumC1 showing a 4-Da mass defect compared to the theoretical mass of the unmodified sequence and exhibiting intense internal fragments and high-intensity b/y fragments before bridged residues R34 and K42. **(B)** Deconvoluted MS/MS spectrum of the same fragment from mRumC1. **(C)** Deconvoluted MS/MS spectrum of an N-terminal fragment of mRumC1 with a 4-Da deficit and specific fragments due to thioether bridges. The inserted spectrum shows the low masses of the same MS/MS spectrum, demonstrating the involvement of A12 and N16 in thioether bridges.

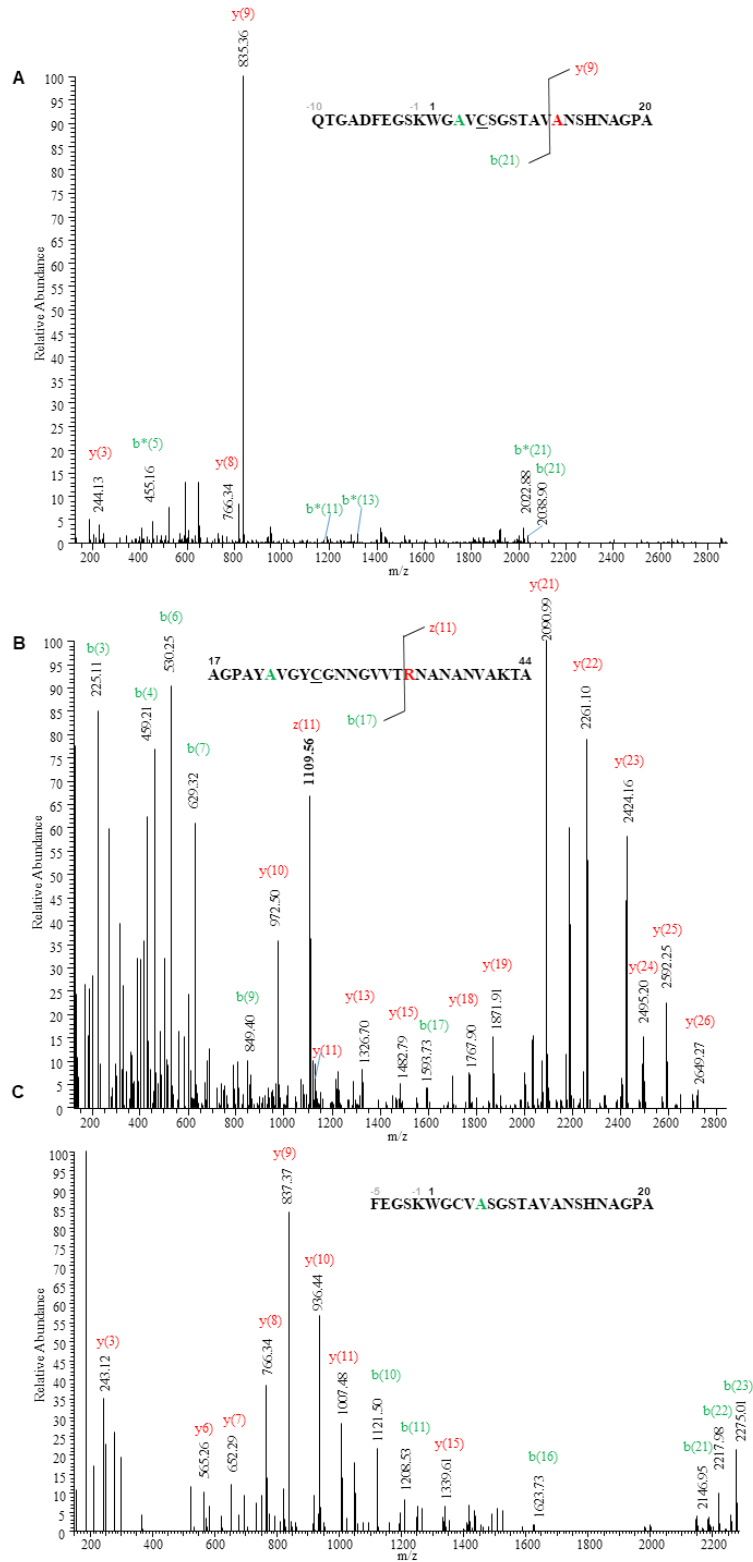


Fig. S5. Tandem mass spectra of mRumC1 mutants from which the residues involved in each thioether bridge were attributed. (see Table S1 for theoretical and observed masses of interest). **(A)** MS/MS spectrum of the Q(-10)-A20 fragment of mRumC1-C3A highlighting the presence of a unique thioether bridge between C5 and A12. The intense y9 fragment highlights the presence of a thioether bridge involving A12. **(B)** MS/MS spectrum of the A17-A44 fragment of mRumC1-C22A highlighting the presence of a unique thioether bridge between C26 and R34. **(C)** MS/MS spectrum of the F(-5)-A20 fragment of mRumC1-C5A revealing alkylation of C3. (b* corresponds to a b fragmentation with a loss of NH3 due to the presence of Q).

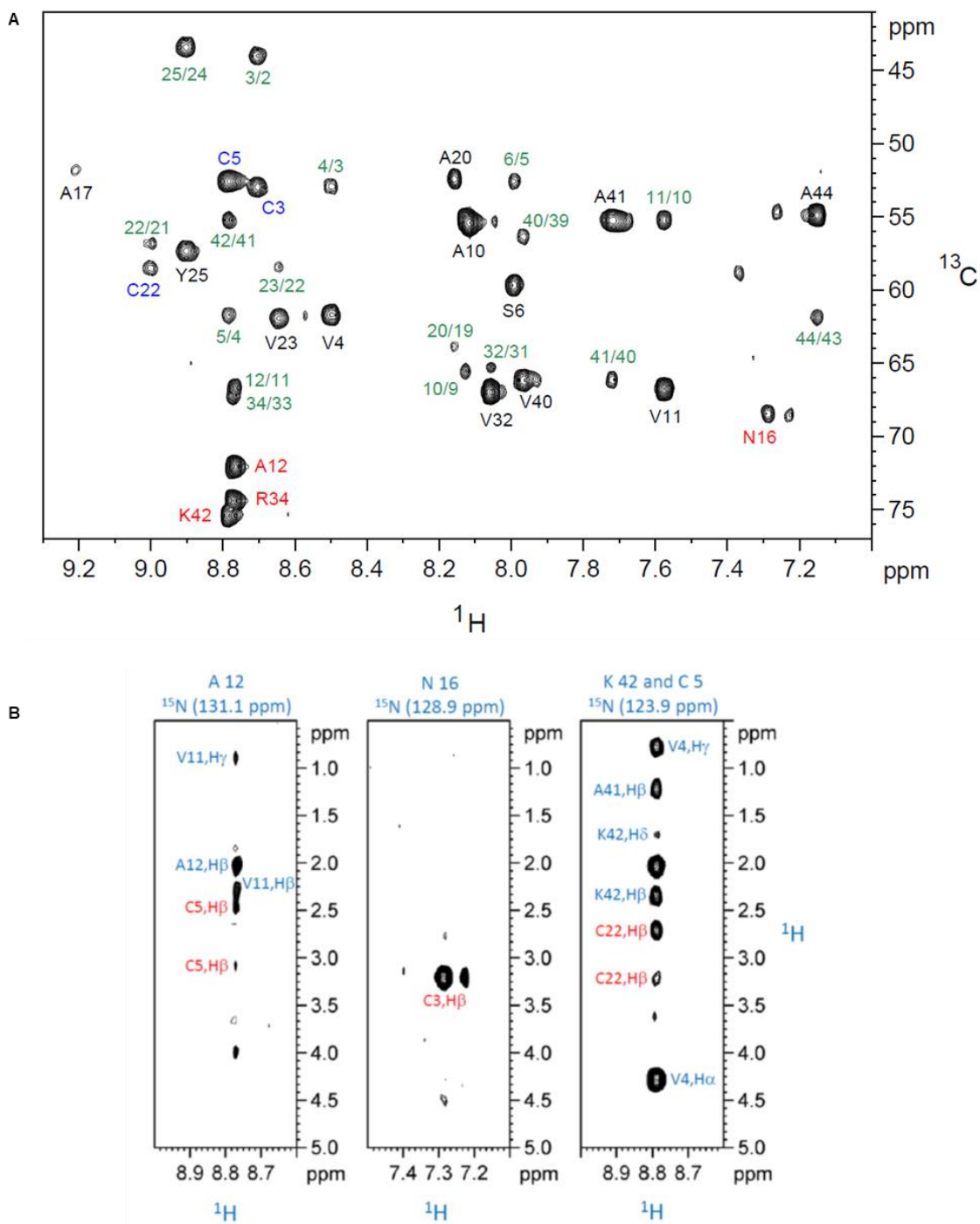


Fig. S6. Determination of the connectivity of the thioether linkages in RumC1 by NMR. (A) Superimposition of ^1H , ^{13}C planes of the HNCA spectrum showing the correlations between amide proton (HN_i) and α -carbons of its own residue ($\text{C}\alpha_i$) and that of the preceding residue ($\text{C}\alpha_{i-1}$). The sequential connectivities ($\text{HN}_i - \text{C}\alpha_{i-1}$) are indicated in green. Amino acids bridged via thioether bonds are shown in red and Cys partners are shown in blue. Note the large downfield shifts at 72.2, 68.6, 74.5 and 75.5 ppm for α -carbons of A12, N16, R34 and K42 residues, respectively. (B) Three $^1\text{H}-^1\text{H}$ strip plots from a ^{15}N -NOESY-HSQC experiment taken at the amide ^{15}N and ^1H chemical shifts of A12, N16, K42 and C5. The backbone NH signals for K42 and C5 are overlapped. The structural connectivities between the β -protons of Cys and the amide protons of residues involved in a thioether bridge are in red (C5-A12, C3-N16 and C22-K42).

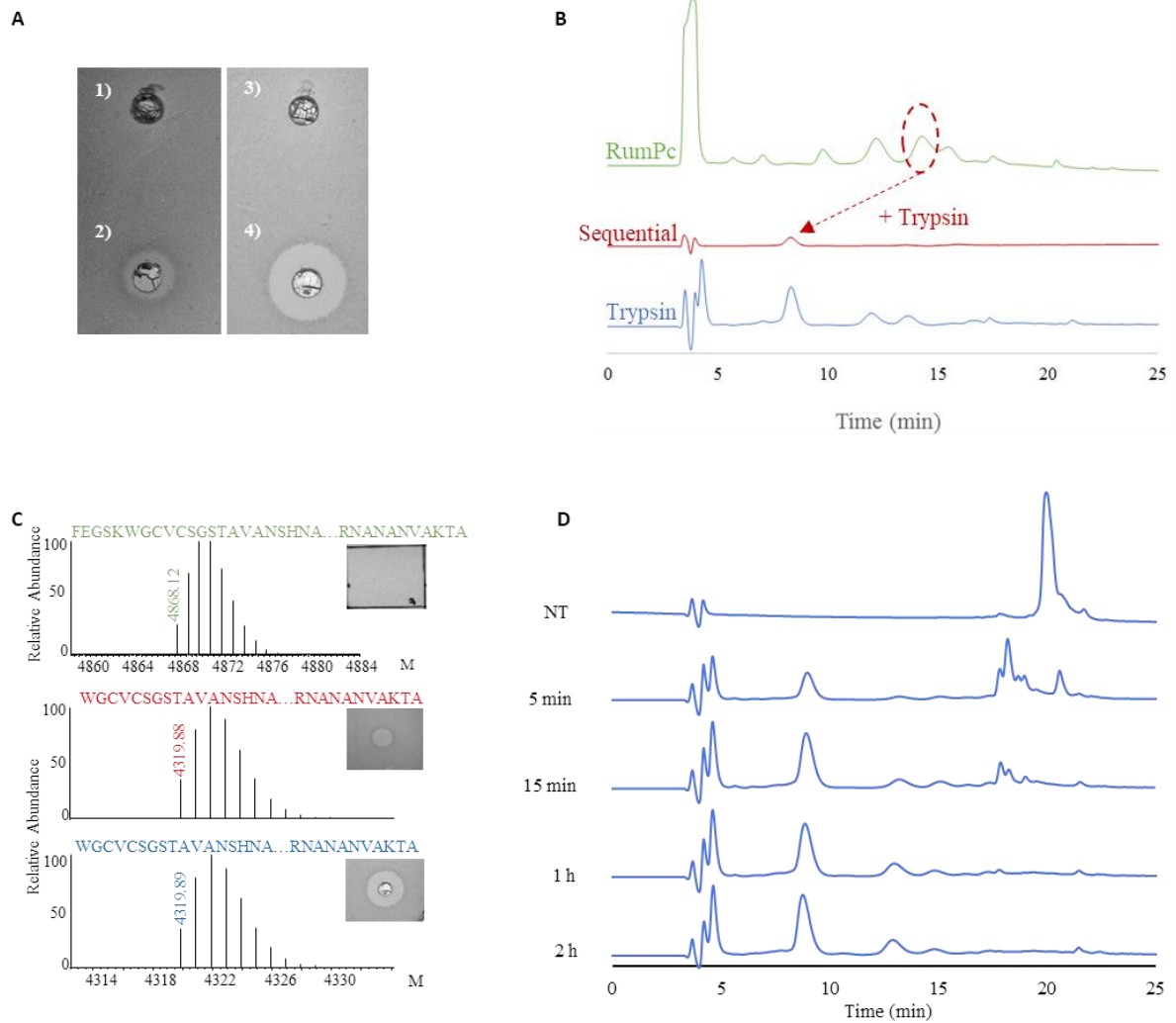


Fig. S7. Cleavage of the leader N-terminal peptides of mRumC1 and anti-Cp activity assays. (A) Anti-Cp activity assays with the different mRumC1 forms, 1: Inactive chemically synthesised unmodified RumC1, 2: Active filtered fraction from the ultrafiltration step used as positive control (see the *in vivo* purification protocol in Fig. 2), 3: Inactive mRumC1, 4: Active mRumC1cc (obtained after cleavage with trypsin). (B) RP-C₁₈ HPLC chromatograms of mRumC1 cleaved with RumPc, sequentially cleaved with RumPc and trypsin, or cleaved by trypsin only. (C) Observed masses of the different cleaved peptide forms and their corresponding anti-Cp activity assays (after RumPc cleavage (top), after RumPc followed by trypsin (middle) and after trypsin alone (bottom)). (D) RP-C₁₈ HPLC chromatograms of a kinetic study for the removal of the leader peptide of mRumC1 (see pic at 20 min) by trypsin leading to the mRumC1cc form (see pic at 9 min), duration of treatment with trypsin is indicated vertically, NT = no treatment. *Peptides were detected at 214 nm in HPLC output.*

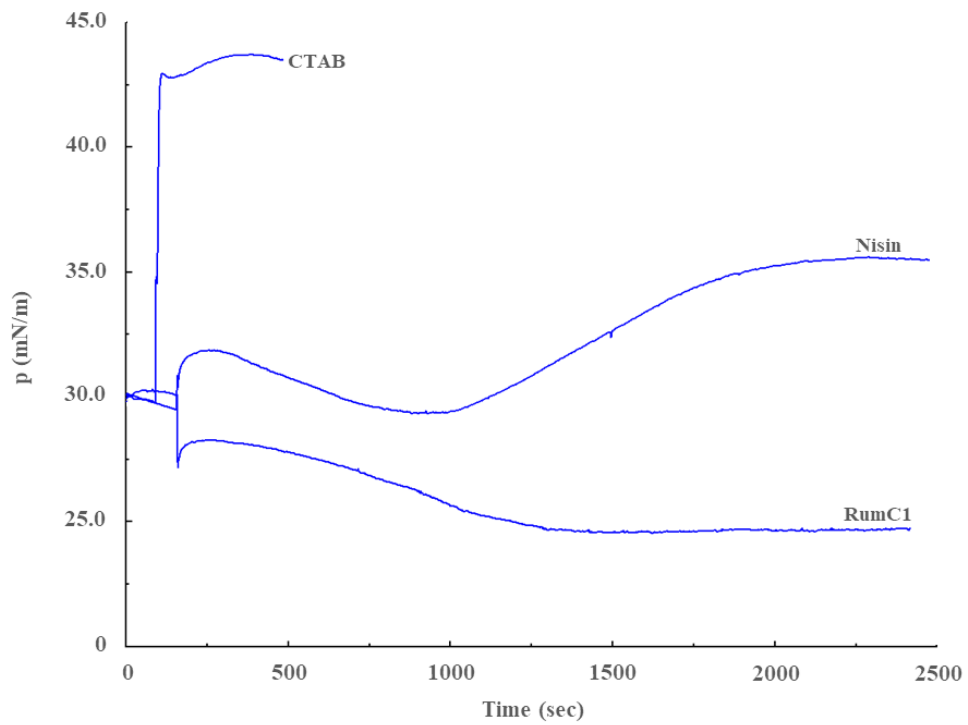
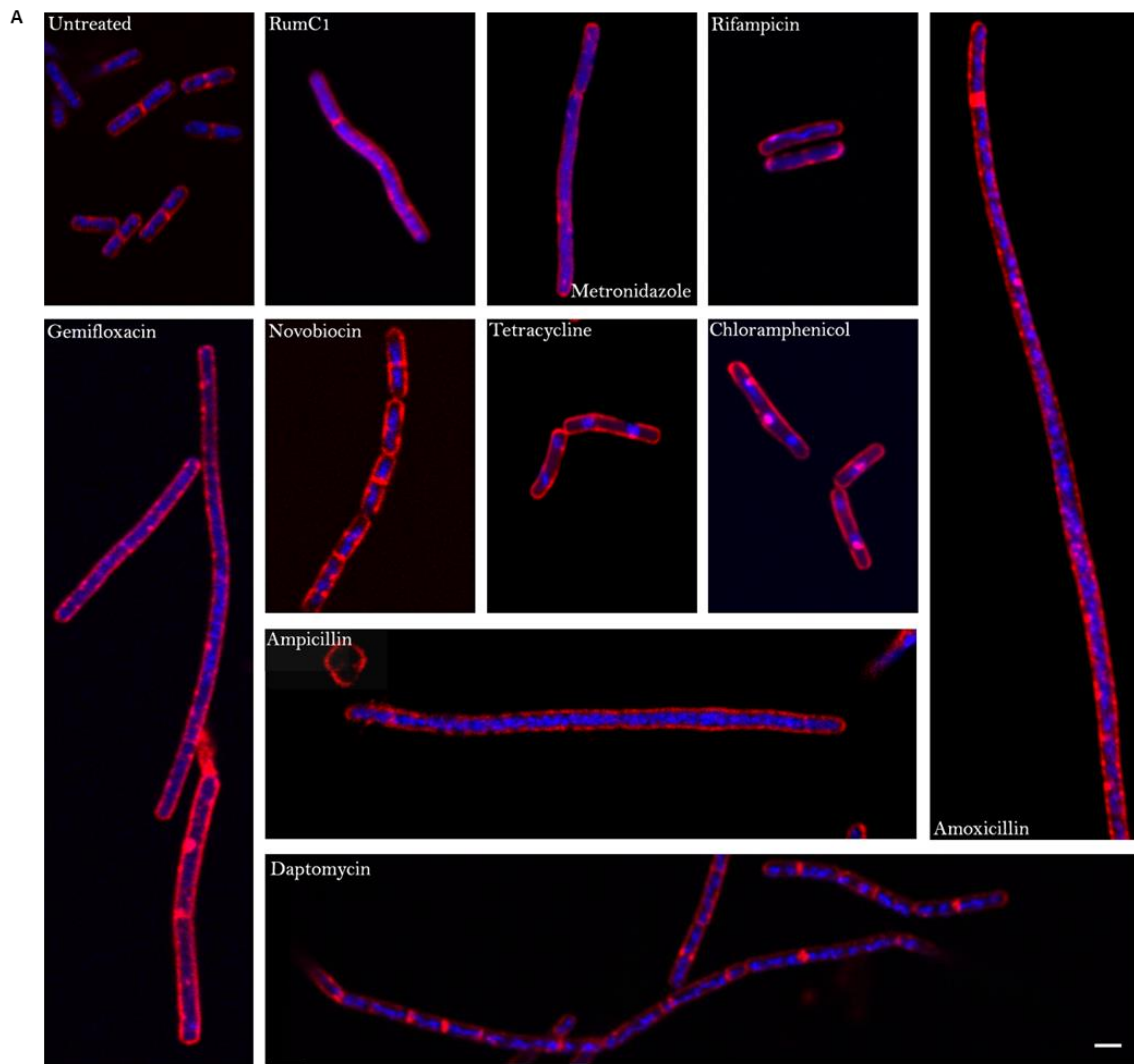


Fig. S8. Evaluation of the ability of RumC1 to insert into bacterial lipids. Total lipids from *C. perfringens* ATCC 13124 were extracted as described in the Supplementary Methods section. Total lipid extract was spread at the air-water interface until the surface pressure (p) reached approximately 30 mN/m. Tested molecules were then injected into the aqueous sub-phase and the insertion into lipids was followed through the continuous measurement of the surface pressure (p). The detergent cetyl trimethylammonium bromide (CTAB) and the pore-forming antimicrobial peptide Nisin were used as positive controls. CTAB was used at 100 μ M whereas Nisin and RumC1 were assayed at 10 x MIC, *i.e.* 7.8 μ M and 15.6 μ M, respectively. Graph shown is representative of three independent experiments.



B

Mode of action	Antibiotics	Length	DNA (C/U)	Filament formation (Y/N)
Control		x 1	C	Not more than 2 cells
Inhibition cell wall synthesis	Amoxicillin	x 14-20	C	N
	Ampicillin	x 5-14	C	N
Inhibition DNA synthesis	Novobiocin	x 1	Hyper C	Y
	Gemifloxacin	x 2-9	U	Y and N
Inhibition RNA synthesis	Rifampicin	x 1-2	50 % hyper C / 50 % U	N
Inhibition protein synthesis	Tetracyclin	x 1-2	Hyper C, circular, 1-3	N
	Chloramphenicol	x 1-4	distinct molecules/cell	N
Loss membrane potential	Daptomycin	x 0.25-4	C	Y
Nucleic acid synthesis	Metronidazole	x 1-4	U with few C spots	Y
				- 2-4 short cells
				- 1 short + 1 long
				- 2 shorts + 1 long in the middle

Fig. S9. Bacterial cytological profiling against Cp. (A) Confocal imaging of untreated and antibiotic-treated Cp cells. Membranes were stained with FM4-64FX and DNA with DAPI. Scale bar = 2 μ m. (B) Description of the phenotypes observed in a. C=condensed, U=uncondensed, Y=yes, N=no. The Length corresponds to 'x times untreated cell-length'.

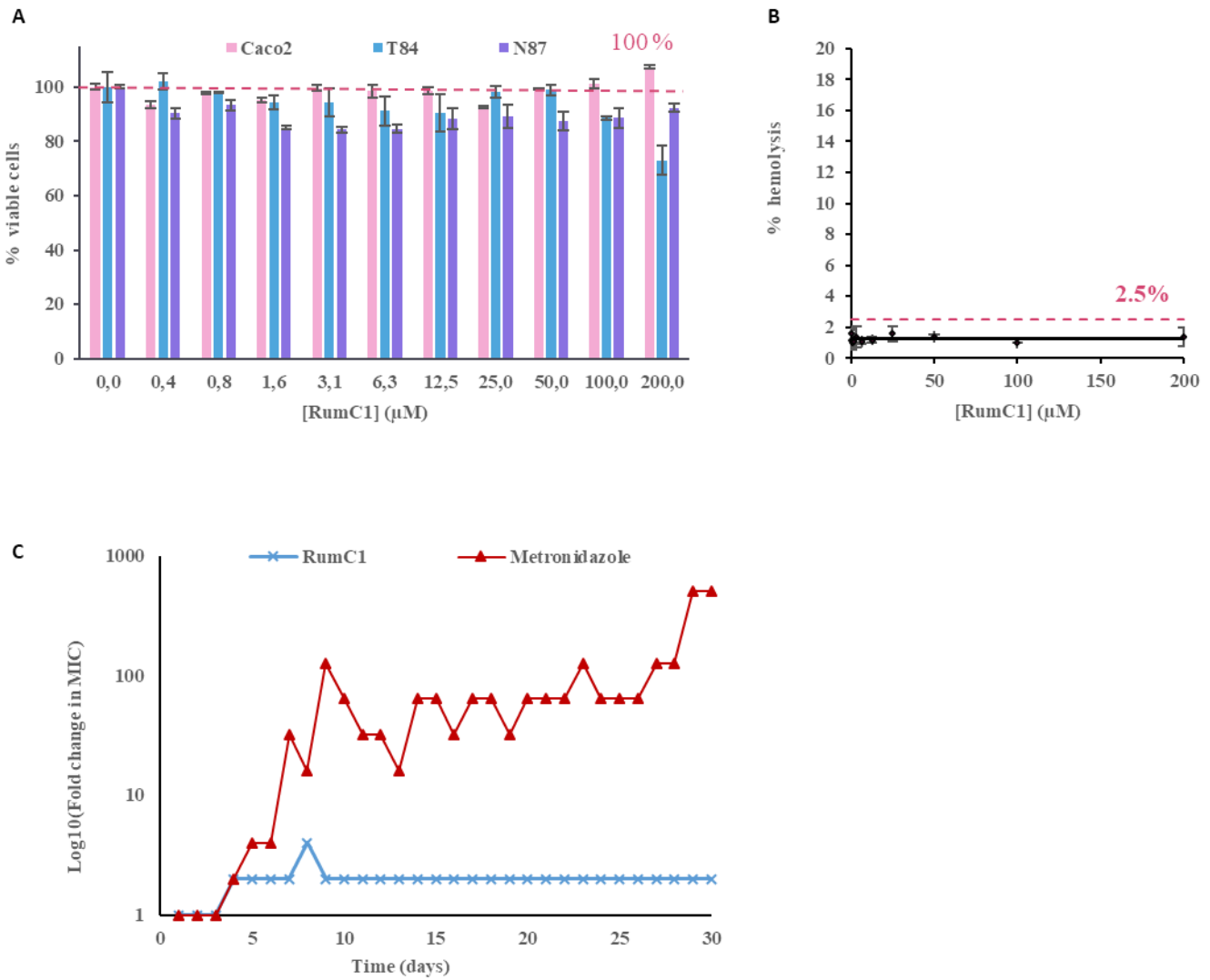


Fig. S10. Assessing RumC1 safety. Human intestinal cell lines (Caco2, T84) and gastric cell lines (N87) (A), and human erythrocytes (B) were incubated with increasing concentrations of RumC1. (A) Cells were incubated with resazurin and conversion into fluorescent resorufin was monitored to determine metabolic activity as an indicator of cell viability, untreated cells were used as a positive control. (B) Haemoglobin release was measured to monitor the lytic activity spectrum of RumC1. Cells incubated with CTAB were used as a positive control for maximum lysis, untreated cells were used as negative control. (C) Induction of resistance to *Cp*, assessed every day over 30 days treatment with RumC1 (blue) or metronidazole (red).

Supplementary Methods

RNA extractions and real-time PCR

RNA was extracted from the faeces of two *R. gnavus* E1 mono-associated rats collected before and after 12 days of colonization. Faecal samples were thawed in 1 mL RNAPro solution containing lysing matrix E (MP Biomedicals). The cells were homogenized in a Fast Prep FP120 cell homogenizer (Thermo Savant) for 2 cycles of 40 s at 6.0 m.s⁻¹. RNA was extracted from the aqueous phase by chloroform extraction and ethanol precipitation before being treated twice with DNase I (NEB). No bacterial RNA could be detected in the faeces of rats before colonization. cDNA was generated using the SuperScript VILO kit (Invitrogen, Thermo Fisher Scientific). Real-time PCR amplification was performed using the LightCycler 480 Instrument and SYBR Green I Master (Roche) on 10 ng cDNA per reaction in the presence of 0.5 μM of each forward and reverse primers (Invitrogen) (fig. S1B). PCR amplification was initiated at 95 °C for 10 min, followed by 45 cycles of 95 °C for 10 s, 60 °C for 10 s and 72 °C for 10 s. A melting curve was added at the end of the amplification to confirm primer specificity. All reactions were performed in duplicate and repeated five times. Fold change in *R. gnavus* E1 transcript amounts was determined using the 2-ΔCt method (58), using *rpoB* as the reference gene.

Peptide synthesis

The linear RumC1 peptide was prepared by solid phase peptide synthesis in an Initiator⁺ Alstra automated microwave assisted synthesizer (Biotage). The peptide was assembled on a Fmoc Ala Wang resin (0.125 mmol scale, 0.53 mmol/g) using standard Fmoc methodologies (59). After assembling, the peptide was manually deprotected and cleaved from the resin by treatment with the mixture TFA/TIS/water (%v/v = 95:2.5:2.5) for 2 h at room temperature and under nitrogen. The resin was filtered out and rinsed with TFA. The filtrate and rinses were combined and reduced under a nitrogen stream. Cold diethyl ether was added to precipitate the crude peptide, which was dissolved in the minimum amount of water and lyophilized. The crude peptide was purified by preparative reversed-phase HPLC in a Phenomenex Jupiter column (250 mm × 21.20 mm, 15 μm, 300 Å) using solvent A (99.9% water/0.1 % TFA) and solvent B (90% ACN/9.9% water/0.1 % TFA). The RumC1 peptide was eluted from the column with a linear gradient from 23.5% to 24.5% B at a flow rate of 10 mL/min. Its purity was checked by analytical reversed-phase HPLC (Phenomenex Jupiter column, 250 mm × 4.6 mm, 15 μm, 300 Å) and it was greater than 98%. The peptide was characterized by Electrospray Ionization-Mass spectrometry (ESI-MS) in positive mode using

an online nano-LC–MS/MS (NCS HPLC, Dionex, and Qexactive HF, Thermo Fisher Scientific).

Site directed mutagenesis of mRumC1

Site directed mutagenesis of the *MBP-RumC1* construct was performed following instructions from the Q5 Site-Directed Mutagenesis Kit (New England BioLabs®). The NEBaseChanger tool was used to generate primer sequences (fig. S1B) and annealing temperatures for each Cys to Ala single mutant. Template plasmids were digested using *DpnI* and were transformed into competent Top10 cells. The mutant plasmids were recovered from cells by using the Wizard® Plus SV Minipreps DNA Purification System (Promega).

Cysteine Alkylation

Ammonium bicarbonate was added to a solution of MBP-mRumC1 (or MBP-mRumC1 mutants) at a concentration of 100 mM. Dithiothreitol was added to this solution at a concentration of 5 mM and subsequently incubated at 55 °C for 35 min. Iodoacetamide was added at a final concentration of 14 mM to alkylate free cysteine and the solution was further incubated at room temperature for 30 min in the dark. To quench unreacted iodoacetamide, dithiothreitol was added to this solution at a concentration of 5 mM and incubating at room temperature for 15 min in the dark. The solution was collected and analysed by LC-MS.

Isotopic labeling of mRumC1

A synthetic plasmid containing the *E. coli* codon-optimized gene of *R. gnavus* E1 encoding RumMc1 (pET-15b-*rumMc1*, ampicillin-resistant) was obtained from Genscript. Plasmids pET-15b-*rumMc1*, pETM-40-*rumC1* and psuf (chloramphenicol-resistant) containing *sufABCDSE* genes were used to transform competent *E. coli* BL21 (DE3) cells. The resulting strain was grown in 3 L of M9 medium containing kan (50 µg/mL), amp (100 µg/mL), chl (34 µg/mL), vitamin B1 (0.5 µg/mL), MgSO₄ (1 mM), FeCl₃ (50 µM) and glucose (4 mg/mL) at 37 °C. At an optical density (OD₆₀₀) of 0.25, cells were harvested by centrifugation (4,000 rpm for 20 min at 4°C). The cells were resuspended in 1 L of labeled minimal medium (Na₂HPO₄ 6 g/L, KH₂PO₄ 3 g/L, ¹⁵NH₄Cl 1 g/L) containing kan (50 µg/mL), amp (100 µg/mL), chl (34 µg/mL), vitamin B1 (0.5 µg/mL), MgSO₄ (1 mM), FeCl₃ (50 µM) and labeled glucose-¹³C (4 mg/mL). The culture was grown at 25°C to an optical density (OD₆₀₀) of 0.8. FeCl₃ (100 µM) and L-cysteine (300 µM) were then added and the culture was induced with 1 mM IPTG. The cells were grown for 15h under stirring and then were harvested by centrifugation (4,000 rpm for 20 min at 4°C). Labeled mRumC1 was purified as described for the unlabeled sample.

NMR of RumC1

NMR experiments were conducted at 27°C, by using a ^{15}N , ^{13}C -labeled RumC1 sample of 0.2 mM in 10 mM phosphate buffer, pH 6.8, in H₂O. NMR data were acquired using a Bruker Avance III 600 MHz spectrometer equipped with a cryogenically cooled triple resonance ($^1\text{H}/^{15}\text{N}/^{13}\text{C}$) 5 mm probe. The following datasets were performed; 2D: [^{15}N , ^1H] HSQC and [^{13}C , ^1H] HSQC; 3D: [^1H , ^{15}N , ^{13}C] HNCACB, CBCA(CO)NH, HNCA, HN(CO)CA, HNCO, HN(CA)CO, ^{15}N -NOESY-HSQC (mixing time of 150 ms) and ^{13}C -TOCSY-HSQC (spin lock of 80 ms).

Lipid insertion assay

Lipid insertion was measured using reconstituted lipid monolayer at the air-water interface as previously described (54, 58). Total lipids were extracted from 3 mL of an overnight culture of *C. perfringens* ATCC 13124 as previously described (58). Extracted total lipids were dried, resolubilized in chloroform:methanol (2:1, v:v) and store at -20 °C under nitrogen. For lipid insertion assay, total lipid extract was spread using a 50 μL Hamilton's syringe at the surface of 700 μL of sterile PBS creating a lipid monolayer at the air-water interface. Lipids were added until the surface pressure reached approximately 30 mN/m, this surface pressure corresponding to a lipid packing density theoretically equivalent to that of the outer leaflet of the cell membrane (54). Lipid insertion of tested molecules was evaluated by injecting them directly into the 700 μL sub-phase of PBS under the lipid monolayer (pH 7.4, volume 800 μL) using a 10 μL Hamilton syringe. Tested molecules were: i) the detergent Cetyl trimethylammonium bromide (CTAB) (at a final concentration of 100 μM), ii) the pore-forming antimicrobial peptide Nisin (at a final concentration of 7.8 μM , corresponding to 10-times its MIC) and iii) RumC1 (at a final concentration of 15.6 μM , corresponding to 10-times its MIC). The variation of the surface pressure caused by the insertion of the molecules into the lipid monolayer was then continuously monitored using a fully automated microtensiometer ($\mu\text{TROUGH SX}$, Kibron Inc., Helsinki, Finland) until reaching equilibrium.